Crystal Structures and Acetonitrile Exchange of Palladium(II) Complexes with Bis(3-aminopropyl)amine and Diethylenetriamine. Effects of Ion-Pair Formation

Takeyoshi Yagyu, Sen-ichi Aizawa, Keiichiro Hatano,† and Shigenobu Funahashi*

Laboratory of Analytical Chemistry, Faculty of Science, Nagoya University, Chikusa, Nagoya 464-01

†Department of Pharmaceutical Sciences, Nagoya City University, Mizuho, Nagoya 467

(Received January 22, 1996)

The crystal structures of palladium(II) complexes with tridentate amine and acetonitrile, $[Pd(CH_3CN)(dptn)](CF_3SO_3)_2$ (**1**) and $[Pd(CH_3CN)(dien)](CF_3SO_3)_2$ (**2**) (dptn = bis(3-aminopropyl)amine and dien = diethylenetriamine), have been determined by X-ray crystal structure analysis. The central palladium(II) ion has a distorted square-planar geometry. The five-membered chelate rings of the dien ligand in **2** are more strained than the six-membered chelate rings of the dptn ligand in **1**, as indicated from the difference in the angles of terminal N–Pd–terminal N and the averaged Pd–N–C angles around the terminal nitrogens. The kinetics of acetonitrile exchange of **1**, **2**, and $[Pd(CH_3CN)(dien)](BF_4)_2$ (**3**) have been investigated by the ^{1}H NMR line-broadening technique. The observed rate constants can be expressed by $k_{obs} = k_1 + k_2$ [CH_3CN] from the dependence of k_{obs} on the acetonitrile concentration. It has been indicated that the k_1 and k_2 paths proceed via the dissociative and associative modes of activation, respectively. The dissociative k_1 path is promoted by the ion-pair formation where the bound ligand effect is enhanced by the electrostatic interaction between the counter anions and amine protons. The reaction mechanisms are discussed in terms of the steric and electronic factors of the bound ligands (dptn and dien) and the effect of the ion-pair formation with the counter anions ($CF_3SO_3^-$ and BF_4^-).

In order to understand the properties of metal complexes in solution and biological systems, the kinetics for ligand-substitution and solvent-exchange reactions of metal complexes have been extensively investigated. The kinetic properties of square-planar palladium(II) and platinum(II) complexes have been well established and an associative mechanism via a trigonal-bipyramidal transition state has been generally accepted.[1)]

As an exceptional instance, the dissociative ligand substitution[2)] and the cis–trans isomerization[3)] were observed for the palladium(II) and platinum(II) complexes with metal–carbon bonds where the large bound ligand effect is operative. In order to clarify the steric and electronic effects of bound ligands on solvent exchange of square-planar Pd(II) and Pt(II) complexes, we have studied the acetonitrile exchange of the Pd(II) complexes with bis(3-aminopropyl)amine (dptn) and diethylenetriamine (dien), which have different chelate-ring size and basicity. In the course of this study, we have found two reaction paths independent of and dependent on the concentration of the free acetonitrile as solvent.[4)] The former reaction path is promoted by increasing the concentration of the counter anion. Consequently, clarification of effects of both bound ligands and counter anions has become necessary.

For the present purpose, we have prepared the Pd(II) complexes with the different tridentate ligands (dptn and dien) and the same counter anion ($CF_3SO_3^-$), $[Pd(CH_3CN)(dptn)](CF_3SO_3)_2$ (**1**) and $[Pd(CH_3CN)(dien)](CF_3SO_3)_2$ (**2**), and the Pd(II) complex with a counter anion (BF_4^-) different from **2** but with the same tridentate ligand, $[Pd(CH_3CN)(dien)](BF_4)_2$ (**3**). The structural characterization of these complexes has been carried out by X-ray crystal structure analyses and ^{1}H NMR spectroscopy. The acetonitrile exchange reaction for these complexes has been investigated by the NMR method. The kinetic difference between **1** and **2**, and **2** and **3** has been discussed in terms of the steric and electronic factors of the bound ligands and counter anions.

Experimental

Materials. Acetonitrile (Wako, Special Grade) was distilled after refluxing for 2 h in the presence of P_2O_5 (ca. 1.4 g dm^{-3}). Deuterated nitromethane (CD_3NO_2, Aldrich) was distilled on a vacuum line, and used both as an inert diluent and as an internal lock substance. Tetrabuthylammonium trifluoromethanesulfonate (n-$Bu_4NCF_3SO_3$, Aldrich) and tetraethylammonium tetrafluoroborate (Et_4NBF_4, Aldrich) were used without further purification in order to vary the concentration of the counter anion.

Preparation of Palladium(II) Complexes. [PdI(dptn)]I. To a solution of $K_2[PdCl_4]$ (39.7 g, 0.122 mol) in hot water was added dptn (19 cm^3, 0.14 mol) with stirring. Into the clear yellow solution was added an aqueous solution of KI (60.6 g, 0.37 mol) with stirring. The resulting precipitate was filtered, then it was washed with water, EtOH, and ether, and finally dried at 70 °C. Yield: 82.3%. Anal. Found: C, 14.79; H, 3.35; N, 8.56%. Calcd for $C_6H_{17}N_3I_2Pd$: C, 14.66; H, 3.49; N, 8.55%.

$[Pd(H_2O)(dptn)](CF_3SO_3)_2$. A small excess of $AgCF_3SO_3$

was added to a suspension of [PdI(dptn)]I (49.2 g, 0.100 mol) in water. The resulting precipitate of AgI was filtered off. The filtrate was concentrated under reduced pressure at 55 °C and then cooled. The resulting crystals were filtered and dried under vacuum. Yield: 65.3%. Anal. Found: C, 17.27; H, 3.32; N, 7.49%. Calcd for $C_8H_{19}N_3PdS_2F_6O_7$: C, 17.35; H, 3.46; N, 7.59%.

[Pd(CH$_3$CN)(dptn)](CF$_3$SO$_3$)$_2$ (1). [Pd(H_2O)(dptn)]-(CF_3SO_3)$_2$ (36.2 g, 6.54×10^{-2} mol) was dissolved in acetonitrile and the water was removed under reflux for about 12 h in the modified Soxhlet extractor with activated Molecular Sieves 4A in the thimble.[5,6] The reflux was repeated twice with freshly activated molecular sieves. The solution was concentrated and filtered under nitrogen. Dichloromethane was added to the filtrate, then the solution was kept at room temperature for a day. The resulting crystals were filtered under nitrogen and dried under vacuum. Yield: 61.6%. Anal. Found: C, 20.75; H, 3.56; N, 9.56%. Calcd for $C_{10}H_{20}N_4PdS_2F_6O_6$: C, 20.82; H, 3.49; N, 9.71%.

[Pd(CH$_3$CN)(dien)](CF$_3$SO$_3$)$_2$ (2). The dien complex **2** was prepared by a procedure similar to that for **1**, using dien instead of dptn. Yield: 68.4%. Anal. Found: C, 17.41; H, 2.81; N, 10.18%. Calcd for $C_8H_{16}N_4PdS_2F_6O_6$: C, 17.51; H, 2.94; N, 10.21%.

[Pd(CH$_3$CN)(dien)](BF$_4$)$_2$ (3). A small excess of $AgBF_4$ was added to a suspension of [PdI(dien)]I (16.5 g, 3.56×10^{-2} mol) in acetonitrile under nitrogen. The resulting precipitate of AgI was filtered off. Dichloromethane was added to the concentrated filtrate, then the solution was kept at room temperature for a day. The resulting crystals were filtered under nitrogen and dried under vacuum. Yield: 42.0%. Anal. Found: C, 16.92; H, 3.81; N, 13.14%. Calcd for $C_6H_{16}N_4PdF_8B_2$: C, 16.99; H, 3.80; N, 13.21%.

X-Ray Structure Determination. The crystals of **1** and **2** suitable for diffraction measurements were obtained by recrystallization from the acetonitrile–dichloromethane solution. Each crystal was sealed in a 0.5-mm o.d. thin wall capillary because the deliquescence of the crystals seriously lowers the quality of the diffraction data. The X-ray diffraction experiments were performed on an Enraf–Nonius CAD4 Kapp diffractometer with graphite-monochromated Mo $K\alpha$ radiation (λ = 0.71073 Å). Least-squares refinement to the setting angles of 25 reflections, collected in the ranges of $20° < 2\theta < 29°$ for **1** and $19° < 2\theta < 23°$ for **2**, led to the cell constants. The intensity data were corrected for the standard Lorentz and polarization effects. The empirical absorption was applied in the case of **2**. The crystallographic data are summarized in Table 1.

The structure was solved by heavy atom methods[7] and refined by difference Fourier and full-matrix least-squares techniques.[8] All non-hydrogen atoms were refined with anisotropic thermal parameters. The hydrogen atoms bound to carbon and nitrogen were included in calculated positions. The atomic scattering factors were taken from the reference.[9]

NMR Sample Preparations and Measurements. The sample preparations for variable-temperature NMR measurements were carried out in a glove box by dissolving weighed quantities of Pd(II) complexes (**1**, **2**, or **3**) and ammonium salts (n-$Bu_4NCF_3SO_3$ or Et_4NBF_4) in the acetonitrile–CD_3NO_2 solution. Each sample solution introduced into a 5 mm o.d. NMR tube was flame-sealed under vacuum after degassing. Variable-temperature ^{1}H NMR measurements were performed on a JEOL JNM-GX270 FT-NMR spectrometer operating at 270 MHz. The temperature was measured by a substitution technique with a thermistor (D641, Takara Thermistor Co.). About 15 min was required for the temperature equilibration of the NMR sample solution and the temperature stability was ±0.2 K.

Table 1. Crystallographic Data for **1** and **2**

	1	**2**
Formula	$PdS_2F_6O_6N_4C_{10}H_{20}$	$PdS_2F_6O_6N_4C_8H_{16}$
Fw	576.8	548.8
Crystal dimensions/mm^3	0.18×0.27×1.26	0.12×0.17×0.54
Crystal system	Monoclinic	Triclinic
Space group	$P2_1/c$	$P\bar{1}$
a/Å	7.964(1)	11.282(2)
b/Å	13.218(1)	12.668(1)
c/Å	20.155(1)	15.324(3)
α/°		93.09(1)
β/°	94.89(1)	92.22(1)
γ/°		114.55(1)
V/Å^3	2113.9(9)	1985(7)
Z	4	4
T/K	293	293
D_c/g cm^{-3}	1.812	1.836
2θ range/°	3—55	3—52.8
Scan technique	ω–2θ	ω–2θ
Scan range (ω/°)	0.90+0.35tan θ	0.75+0.35tan θ
Criterion for observation	$F_o > 3\sigma(F_o)$	$F_o > 3.5\sigma(F_o)$
Unique obsed data	3940	5024
No. of variables	262	487
μ/cm^{-1}	11.38	12.07
R[a]	0.068	0.098
R_w[a]	0.053	0.076

a) $R = \sum||F_o| - |F_c||/\sum|F_o|$. $R_w = [\sum w\ (|F_o| - |F_c|)^2/\sum w\ |F_o|^2]^{1/2}$ where $w = 1/\sigma^2$.

Results and Discussion

Crystal Structures of 1 and 2. The perspective views of **1** and **2** are displayed in Figs. 1 and 2, respectively, along with the atomic numbering scheme. Two sets of independent molecules with a slight difference in their structures are included in the asymmetric unit for **2**. A list of fractional atomic constants and isotropic thermal parameters are given

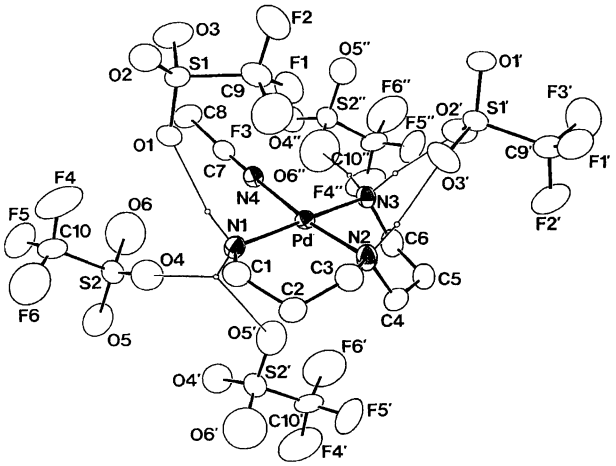

Fig. 1. Crystal structure of [Pd(CH$_3$CN)(dptn)](CF$_3$SO$_3$)$_2$ (**1**). Thermal ellipsoids are at the 20% probability level. All hydrogen atoms except for those with hydrogen bonding are omitted for clarity. Hydrogen atoms are shown as spheres of arbitrary size and hydrogen bonds are represented by narrow lines.

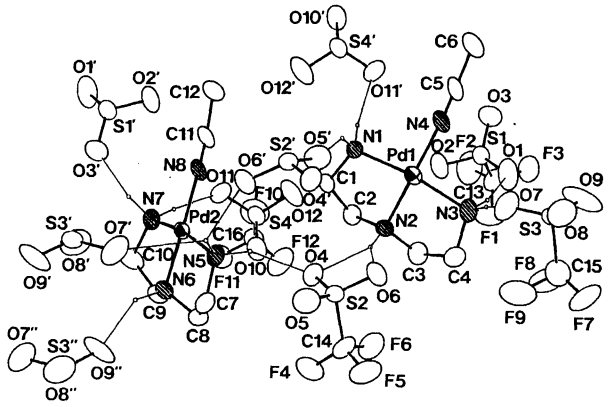

Fig. 2. Crystal structure of $[Pd(CH_3CN)(dien)](CF_3SO_3)_2$ (**2**). Thermal ellipsoids are at the 20% probability level. All hydrogen atoms except for those with hydrogen bonding are omitted for clarity. Hydrogen atoms are shown as spheres of arbitrary size and hydrogen bonds are represented by narrow lines.

in Table 2 for **1** and in Table 3 for **2**. The selected bond distances and angles for **1** and **2** are listed in Tables 4 and 5, respectively.[10]

Table 2. Fractional Atomic Constants and Isotropic Thermal Parameters for $[Pd(CH_3CN)(dptn)](CF_3SO_3)_2$ (**1**)

Atom	x	y	z	B_{eq}/Å^{2} a)
Pd	0.20784(6)	0.20297(4)	0.11594(3)	3.85(1)
S1	0.0756(3)	−0.0240(2)	0.2913(1)	6.15(6)
S2	0.3875(3)	−0.1524(2)	0.0293(1)	6.07(6)
F1	−0.0253(7)	0.1494(5)	0.2448(3)	10.2(2)
F2	−0.054(1)	0.1283(5)	0.3459(3)	14.4(3)
F3	0.1785(9)	0.1574(5)	0.3127(4)	15.4(3)
F4	0.321(1)	−0.2414(8)	0.1351(4)	19.5(4)
F5	0.374(1)	−0.3360(6)	0.0568(6)	19.7(5)
F6	0.571(1)	−0.2565(8)	0.1102(5)	22.0(5)
O1	0.1872(7)	−0.0300(4)	0.2394(3)	7.6(2)
O2	0.1401(7)	−0.0537(5)	0.3565(3)	9.8(2)
O3	−0.0890(8)	−0.0625(5)	0.2742(4)	11.0(3)
O4	0.426(1)	−0.0664(5)	0.0714(4)	13.2(3)
O5	0.509(1)	−0.1716(5)	−0.0138(3)	14.1(3)
O6	0.223(1)	−0.1618(7)	0.0086(5)	18.5(4)
N1	0.3893(7)	0.1051(4)	0.1547(3)	4.8(1)
N2	0.3300(7)	0.3344(5)	0.1424(3)	5.9(2)
N3	0.0273(7)	0.2914(4)	0.0676(3)	4.9(1)
N4	0.0652(7)	0.0803(4)	0.0950(3)	4.5(2)
C1	0.5304(9)	0.1380(7)	0.2036(4)	6.2(2)
C2	0.589(1)	0.2425(7)	0.1892(4)	6.7(3)
C3	0.472(1)	0.3236(7)	0.1980(5)	7.1(3)
C4	0.374(1)	0.3934(7)	0.0851(4)	6.6(3)
C5	0.227(1)	0.4279(7)	0.0407(5)	7.2(3)
C6	0.098(1)	0.3518(7)	0.0145(4)	7.2(3)
C7	−0.0142(9)	0.0104(6)	0.0921(4)	4.8(2)
C8	−0.119(1)	−0.0788(7)	0.0894(5)	7.9(3)
C9	0.044(1)	0.1087(9)	0.3002(5)	7.1(3)
C10	0.425(2)	−0.247(1)	0.0936(8)	10.3(5)

a) Anisotropically refined atoms are given in the form of the isotropic equivalent displacement parameter defined as: (4/3) $\times\{a^2B(1,1)+b^2B(2,2)+c^2B(3,3)+ab(\cos\gamma)B(1,2)+ac(\cos\beta)\times B(1,3)+bc(\cos\alpha)B(2,3)\}$.

Table 3. Fractional Atomic Constants and Isotropic Thermal Parameters for $[Pd(CH_3CN)(dien)](CF_3SO_3)_2$ (**2**)

Atom	x	y	z	B_{eq}/Å^{2} a)
Pd1	0.0999(1)	0.3001(1)	0.29176(8)	5.75(5)
Pd2	0.0267(1)	0.2935(1)	0.77024(7)	5.15(4)
S1	0.2662(5)	0.1318(4)	0.1548(3)	7.3(2)
S2	0.2121(4)	0.6145(4)	0.5127(3)	5.8(1)
S3	0.1737(5)	0.6105(5)	0.0642(3)	7.3(2)
S4	0.2294(5)	0.1142(5)	0.6585(3)	7.1(2)
F1	0.515(2)	0.206(2)	0.188(1)	16.9(8)
F2	0.410(2)	0.029(2)	0.193(1)	16(1)
F3	0.443(2)	0.100(3)	0.071(2)	13.8(7)
F4	0.413(3)	0.725(3)	0.622(1)	13.9(8)
F5	0.406(4)	0.813(2)	0.511(3)	14(1)
F6	0.457(2)	0.676(3)	0.497(2)	14.1(8)
F7	0.388(3)	0.799(2)	0.064(2)	15.9(6)
F8	0.410(2)	0.666(2)	0.121(3)	15.2(7)
F9	0.320(3)	0.754(3)	0.180(1)	21.2(8)
F10	0.337(2)	−0.023(2)	0.685(3)	13.6(7)
F11	0.381(2)	0.111(2)	0.785(1)	15.2(7)
F12	0.472(2)	0.144(2)	0.667(1)	17.1(9)
O1	0.297(2)	0.240(1)	0.1158(8)	12.3(7)
O2	0.247(1)	0.1381(9)	0.2451(7)	8.6(5)
O3	0.179(1)	0.034(1)	0.1038(8)	10.6(5)
O4	0.204(1)	0.5093(9)	0.5487(7)	8.3(4)
O5	0.145(1)	0.666(1)	0.5586(9)	10.2(5)
O6	0.196(1)	0.601(1)	0.4204(7)	8.3(5)
O7	0.123(1)	0.552(1)	0.137(1)	12.6(6)
O8	0.103(1)	0.673(1)	0.045(1)	13.1(7)
O9	0.195(1)	0.557(2)	−0.003(1)	21(1)
O10	0.275(1)	0.237(1)	0.6752(8)	10.4(5)
O11	0.127(1)	0.049(1)	0.7095(8)	9.7(5)
O12	0.214(1)	0.071(1)	0.5701(7)	10.6(6)
N1	−0.009(1)	0.197(1)	0.3838(8)	6.5(4)
N2	0.236(1)	0.373(1)	0.3895(8)	6.3(5)
N3	0.242(1)	0.406(1)	0.2163(8)	8.1(6)
N4	−0.035(2)	0.224(1)	0.1957(8)	7.1(6)
N5	0.048(1)	0.440(1)	0.7089(8)	5.5(4)
N6	0.168(1)	0.406(1)	0.8511(8)	6.0(5)
N7	0.044(1)	0.168(1)	0.8416(8)	6.2(5)
N8	−0.119(1)	0.179(1)	0.6912(8)	5.8(5)
C1	0.077(2)	0.227(1)	0.4681(9)	6.7(6)
C2	0.220(2)	0.275(1)	0.449(1)	6.2(6)
C3	0.366(2)	0.414(2)	0.350(1)	8.2(7)
C4	0.354(2)	0.492(1)	0.278(1)	8.0(7)
C5	−0.111(2)	0.170(1)	0.144(1)	7.2(8)
C6	−0.215(2)	0.099(2)	0.077(1)	10.6(9)
C7	0.149(2)	0.540(1)	0.762(1)	7.7(7)
C8	0.245(2)	0.505(1)	0.803(1)	7.1(6)
C9	0.246(2)	0.339(2)	0.888(1)	7.9(7)
C10	0.144(2)	0.229(2)	0.916(1)	10.2(9)
C11	−0.198(2)	0.113(1)	0.651(1)	6.1(7)
C12	−0.312(2)	0.019(1)	0.601(1)	7.6(7)
C13	0.422(2)	0.120(2)	0.152(2)	9.2(5)
C14	0.381(3)	0.708(3)	0.541(2)	10.7(7)
C15	0.333(2)	0.712(2)	0.0946(6)	13.5(4)
C16	0.367(2)	0.088(3)	0.700(2)	9.3(5)

a) Anisotropically refined atoms are given in the form of the isotropic equivalent displacement parameter defined as: (4/3) $\times\{a^2B(1,1)+b^2B(2,2)+c^2B(3,3)+ab(\cos\gamma)B(1,2)+ac(\cos\beta)\times B(1,3)+bc(\cos\alpha)B(2,3)\}$.

Table 4. Selected Bond Distances (Å) and Angles (deg) for $[Pd(CH_3CN)(dptn)](CF_3SO_3)_2$ (**1**)

	Bond distances		
Pd–N1	2.045(1)	C2–C3	1.44(1)
Pd–N2	2.039(6)	C4–C5	1.48(1)
Pd–N3	2.036(5)	C5–C6	1.50(1)
Pd–N4	2.004(6)	C7–C8	1.44(1)
N1–C1	1.494(9)	N1–O4	2.85
N2–C3	1.53(1)	N1–O1	3.03
N2–C4	1.46(1)	N1–O5′ [a]	3.14
N3–C6	1.48(1)	N2–O3′ [b]	2.99
N4–C7	1.119(9)	N3–O2′ [b]	2.94
C1–C2	1.49(1)	N3–O6″ [c]	2.96
	Bond angles		
N1–Pd–N2	97.6(2)	Pd–N3–C6	111.0(5)
N1–Pd–N3	173.5(2)	Pd–N4–C7	170.9(6)
N1–Pd–N4	86.5(2)	N1–C1–C2	111.7(6)
N2–Pd–N3	86.4(2)	C1–C2–C3	116.8(7)
N2–Pd–N4	173.4(2)	N2–C3–C2	115.1(7)
N3–Pd–N4	90.0(2)	N3–C4–C5	114.1(7)
Pd–N1–C1	122.4(5)	C4–C5–C6	119.2(7)
Pd–N2–C3	114.7(5)	N3–C6–C5	113.4(7)
Pd–N2–C4	112.9(5)	N4–C7–C8	178.8(8)
C3–N2–C4	114.6(6)		

Following equivalent positions: a) $1-x, -y, -z$, b) $-x, 1/2+y, 1/2-z$, c) $-x, -y, -z$.

Table 5. Selected Bond Distances (Å) and Angles (deg) for $[Pd(CH_3CN)(dien)](CF_3SO_3)_2$ (**2**)

	Bond distances		
Pd1–N1	2.05(1)	C1–C2	1.52(3)
Pd1–N2	1.99(1)	C3–C4	1.55(3)
Pd1–N3	2.05(1)	C5–C6	1.47(2)
Pd1–N4	1.97(1)	C7–C8	1.48(3)
Pd2–N5	2.05(1)	C9–C10	1.49(2)
Pd2–N6	1.97(1)	C11–C12	1.48(2)
Pd2–N7	2.05(1)	N1–O5′ [a]	2.88
Pd2–N8	1.99(1)	N1–O11′ [b]	3.07
N1–C1	1.51(2)	N2–O4	3.04
N2–C2	1.52(2)	N2–O6	3.13
N2–C3	1.50(2)	N3–O1	2.83
N3–C4	1.53(2)	N3–O7	2.97
N4–C5	1.11(2)	N5–O4	3.03
N5–C7	1.47(2)	N5–O6′ [a]	3.18
N6–C8	1.45(2)	N5–O7′ [a]	3.13
N6–C9	1.56(2)	N6–O9″ [c]	2.78
N7–C10	1.50(2)	N7–O11	2.87
N8–C11	1.08(2)	N7–O3′ [b]	2.94
	Bond angles		
N1–Pd1–N2	85.0(5)	Pd1–N4–C5	173(2)
N1–Pd1–N3	167.8(5)	Pd2–N5–C7	107(1)
N1–Pd1–N4	94.0(5)	Pd2–N6–C8	108.1(9)
N2–Pd1–N3	84.1(4)	Pd2–N6–C9	106.1(9)
N2–Pd1–N4	178.2(7)	C8–N6–C9	114(1)
N3–Pd1–N4	96.7(5)	Pd2–N7–C10	107(1)
N5–Pd2–N6	82.9(5)	Pd2–N8–C11	176(2)
N5–Pd2–N7	168.0(5)	N1–C1–C2	110(1)
N5–Pd2–N8	97.6(5)	N2–C2–C1	104(2)
N6–Pd2–N7	86.0(6)	N2–C3–C4	103(2)
N6–Pd2–N8	178.5(5)	N3–C4–C3	102(1)
N7–Pd2–N8	93.6(5)	N4–C5–C6	178(2)
Pd1–N1–C1	107.4(8)	N5–C7–C8	110(2)
Pd1–N2–C2	105.4(8)	N6–C8–C7	104(1)
Pd1–N2–C3	106.7(9)	N6–C9–C10	105(2)
C2–N2–C3	110(2)	N7–C10–C9	110(1)
Pd1–N3–C4	108(1)	N8–C11–C12	176(2)

Following equivalent positions: a) $-x, 1-y, 1-z$, b) $-x, -y, 1-z$, c) $x, y, 1+z$.

Though each Pd(II) complex cation has a square-planar geometry, an apparent difference in distortion around Pd(II) is observed between **1** and **2**. For example, the N1–Pd1–N3 and N5–Pd2–N7 angles in **2** (167.8(5) and 168.0(5)°, respectively) are clearly smaller than the N1–Pd–N3 angle in **1** (186.5(2)°). Furthermore, the averaged Pd–N–C angle around the terminal nitrogen donor atoms of the tridentate amine ligands of **2** (107.0°) is appreciably smaller than that of **1** (115.3°), which is comparable to the Pt–N–C angles of the monodentate primary amine ligand for the square-planar Pt(II) complexes.[11,12] Such distortion of **1** arises from the relatively small ring size of the five-membered chelate ring for the dien ligand in comparison with the six-membered chelate ring for the dptn ligand.

The crystal structures for **1** and **2** consist of the network of hydrogen bonds between amine protons and oxygen atoms of $CF_3SO_3^-$ as shown in Figs. 1 and 2 (N1–O4 = 2.85, N1–O1 = 3.03, N1–O5′ = 3.14, N2–O3′ = 2.99, N3–O2′ = 2.94, and N3–O6″ = 2.96 Å for **1** and N1–O5′ = 2.88, N1–O11′ = 3.07, N2–O4 = 3.04, N2–O6 = 3.13, N3–O1 = 2.83, N3–O7 = 2.97, N5–O4 = 3.03, N5–O6′ = 3.18, N5–O7′ = 3.13, N6–O9″ = 2.78, N7–O11 = 2.87, and N7–O3′ = 2.94 Å for **2**). The existence of the network of hydrogen bonds implies that there is ion-pair formation in the solution via hydrogen bonding (vide infra).

It is worth noting that the Pd–N distance for the linearly coordinated acetonitrile in **1** (2.004(6) Å) is a little longer than those in **2** (Pd1–N4 = 1.97(1) and Pd2–N8 = 1.99(1) Å). This finding is consistent with the higher basicity of the dptn ligand compared with the dien ligand ($pK_{a1} = 7.69$, and $pK_{a2} = 9.57$, and $pK_{a3} = 10.65$ for dptn[13] and $pK_{a1} = 4.23$, $pK_{a2} = 9.02$, and $pK_{a3} = 9.84$ for dien[14] at 25 °C and $I = 0.1$ mol dm^{-3} in aqueous solution) which brings about the stronger donation to the Pd(II) ion, and consequently the greater bound ligand effect.

^{1}H NMR Spectra. The ^{1}H NMR spectrum of the solution of **3** is shown in Fig. 3 as a representative. Each sample solution for **1**, **2**, and **3** shows ^{1}H NMR peaks corresponding to methyl groups for the bound and free acetonitrile, methylene and amine protons for the tridentate ligands, and ethyl or *n*-buthyl groups for Et_4NBF_4 or *n*-$Bu_4NCF_3SO_3$ (Table 6).

The ^{1}H NMR signals of the amine protons in the ligand for each complex shift downfield with an increase in the concentration of the counter anion, BF_4^- or $CF_3SO_3^-$, at the constant concentrations of the Pd(II) complex and free acetonitrile. For an example, Fig. 4(a) shows the dependence of the chemical shift of the secondary amine proton on the total

Table 6. ^{1}H NMR Chemical Shifts of the Sample Solutions for **1**, **2**, and **3**

Complex	δ (relative to TMS)				
	Free CH_3CN	Bound CH_3CN	Methylene	Amine [a]	R_4N^+ [b]
1	2.0 (s)	2.47 (s)	1.8—2.2 (m)	3.61—3.89 (s, NH_2)	0.98 (t)
			2.7—2.9 (m)	3.91— (s, NH_2)[c]	1.3—1.5 (m)
				4.66—5.10 (s, NH)	1.7—1.8 (m)
					3.2—3.3 (m)
2	2.0 (s)	2.43 (s)	2.8—2.9 (m)	4.19— (s, NH_2)[c]	0.99 (t)
			3.2—3.4 (m)	4.51—4.68 (s, NH_2)	1.3—1.5 (m)
				6.30—6.60 (s, NH)	1.6—1.8 (m)
					3.2—3.3 (m)
3	2.0 (s)	2.43 (s)	2.8—2.9 (m)	4.10—4.17 (s, NH_2)	1.3 (t)
			3.2—3.4 (m)	— (NH_2)[c]	3.3 (q)
				5.81—5.91 (s, NH)	

a) The range of chemical shifts with an increase in the concentration of counter anion. b) R = *n*-Bu for **1** and **2**, and R = Et for **3**. c) Blank denotes overlapping with the peak of CD_2HNO_2 (4.3 ppm).

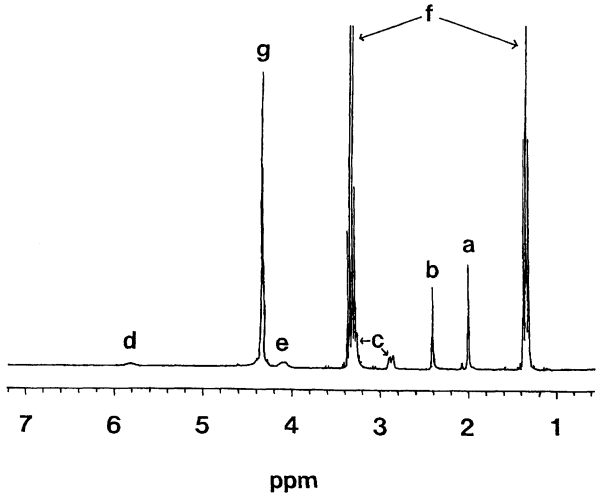

Fig. 3. ^{1}H NMR spectrum of the solution of [Pd(CH_3CN)-(dien)](BF_4)$_2$ (**3**). (a) free CH_3CN, (b) bound CH_3CN, (c) methylene protons of dien, (d) primary amine protons of dien, (e) secondary amine proton of dien, (f) methyl and methylene protons of Et_4N^+, (g) CHD_2NO_2.

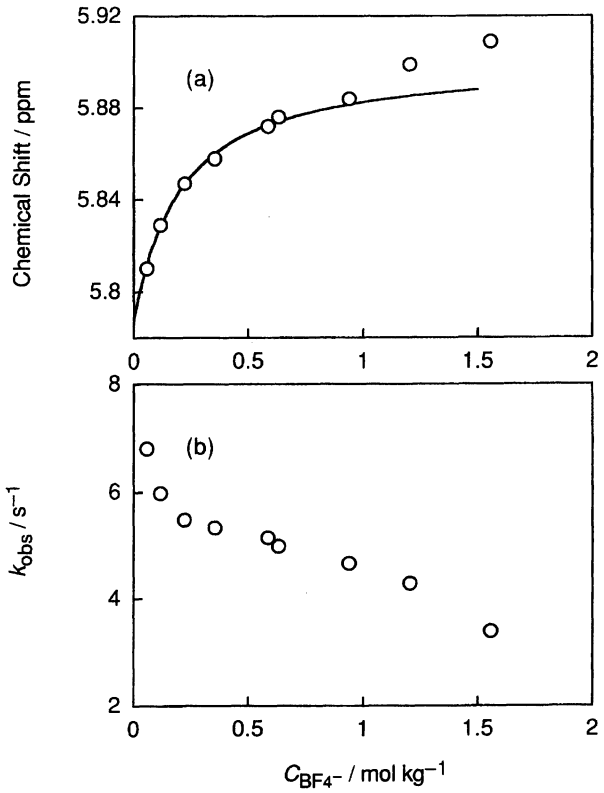

Fig. 4. (a) Dependence of the chemical shift of the secondary amine proton for **3** on the total concentration of BF_4^- (C_{BF_4-}) at 312 K. The curve is depicted by using the recalculated formation constant for the 1 : 1 ion pair, $K_1 = 5.7 \pm 1.1$ kg mol^{-1} (Ref. 4). (b) Dependence of k_{obs} for **3** on the total concentration of BF_4^- (C_{BF_4-}) at 312 K. [complex] = (2.9—3.0)$\times 10^{-2}$ mol kg^{-1} and [CH_3CN] = (3.3—3.4)$\times 10^{-2}$ mol kg^{-1}.

concentration of BF_4^- (C_{BF_4-}) for **3**. Each chemical shift of the amine protons for **1**, **2**, and **3** approaches a limiting value followed by further gradual downfield shift. Such a change in chemical shift can be ascribed to the ion-pair formation between the Pd(II) complex and counter anion because of the deshielding of the amine protons due to the electrostatic interaction with a negative charge on the counter anion. This is supported by the existence of the network of hydrogen bonding in the crystal structures for **1** and **2** (vide supra). Considering the dielectric constant of 35.87 (30 °C and 1 atm) for nitromethane,[15] the downfield shift at the first step corresponds to the formation of the 1 : 1 ion pair, and the following gradual downfield shift corresponds to the 1 : 2 ion pair formation. The two-step variation in the chemical shift which is also observed for the variation in the observed rate constants (vide infra) as shown in Fig. 4(b) indicate that the 1 : 1 ion pair for **3** forms quantitatively at C_{BF_4-} = 0.8 mol kg^{-1}. Similarly it has been revealed that the 1 : 1 ion pairs for **1** and **2** form quantitatively at $C_{CF_3SO_3-}$ = 0.39 and 0.34 mol kg^{-1}, respectively, under the conditions where

the counter anion is in a large excess relative to the Pd(II) complex.

Kinetics of Acetonitrile Exchange. Over the temperature range of NMR measurements of each sample (289.2—305.3 K for **1**, 309.3—324.8 K for **2**, and 313.2—328.9 K for **3**), the two-site exchange between free and bound acetonitrile was observed without change in chemical shift. The observed first-order rate constant k_{obs} is given by Eq. 1:

$$k_{obs} = \pi(\Delta\nu_{obs} - \Delta\nu_{ref})[CH_3CN]/[b\text{-}CH_3CN] \quad (1)$$

where $\Delta\nu_{obs}$ and $\Delta\nu_{ref}$ are the half-height widths of the free acetonitrile in the presence and absence, respectively, of the Pd(II) complex, and $[CH_3CN]$ and $[b\text{-}CH_3CN]$ are the concentrations of the free and bound acetonitrile, respectively.

Preliminary experiments revealed that the observed rate constant can be expressed by Eq. 2:

$$k_{obs} = k_1 + k_2[CH_3CN] \quad (2)$$

because plots of k_{obs} versus $[CH_3CN]$ lie on a straight line with a significant intercept for each complex. The value of k_{obs} is quite changeable by the concentration of the counter anion, as k_1 tends to increase and k_2 tends to decrease with increasing the concentration of the counter anion. Therefore, we selected the conditions for kinetic measurements where the 1 : 1 ion pair forms quantitatively in order to compare the results for each complex to one another.

The dependence of k_{obs} on $[CH_3CN]$ at various temperatures for **1**, **2**, and **3** is shown in Fig. 5. The rate constants k_1 and k_2 are expressed by Eqs. 3 and 4, respectively, according to the transition-state theory,

$$k_1 = (k_B T/h)\exp(-\Delta H_1^{\ddagger}/RT + \Delta S_1^{\ddagger}/R) \quad (3)$$

$$k_2 = (k_B T/h)\exp(-\Delta H_2^{\ddagger}/RT + \Delta S_2^{\ddagger}/R) \quad (4)$$

where $\Delta H_1^{\ddagger}$ and $\Delta H_2^{\ddagger}$ are the activation enthalpies and $\Delta S_1^{\ddagger}$ and $\Delta S_2^{\ddagger}$ are the activation entropies for k_1 and k_2 paths, respectively. The activation parameters for each complex were obtained by applying a simultaneous least-squares fitting to Eqs. 2, 3, and 4, as listed in Table 7. It has been confirmed by the reexamination of the acetonitrile exchange of $[Pd(CH_3CN)_4](BF_4)_2$ that there is no contribution of the k_1 path for the $[Pd(CH_3CN)_4](BF_4)_2$ system, as reported by Merbach et al.[1d]

The k_2 path dependent on the concentration of the free acetonitrile can be assigned to the associative mechanism because of the rather large negative values of $\Delta S_2^{\ddagger}$, as generally observed for the square-planar Pd(II) complexes. This assignment is supported by the fact that the activation parameters for the k_2 path are comparable to those for the associative acetonitrile exchange of $[Pd(CH_3CN)_4](BF_4)_2$, which proceeds only by the k_2 path (see Table 7). On the other hand, considering that the k_1 path independent of the concentration of the free acetonitrile is not observed for the acetonitrile exchange of $[Pd(CH_3CN)_4](BF_4)_2$ which has the same counter anion as **3**, the k_1 path may proceed via a dissociative activation mode promoted by the effects of the bound tridentate

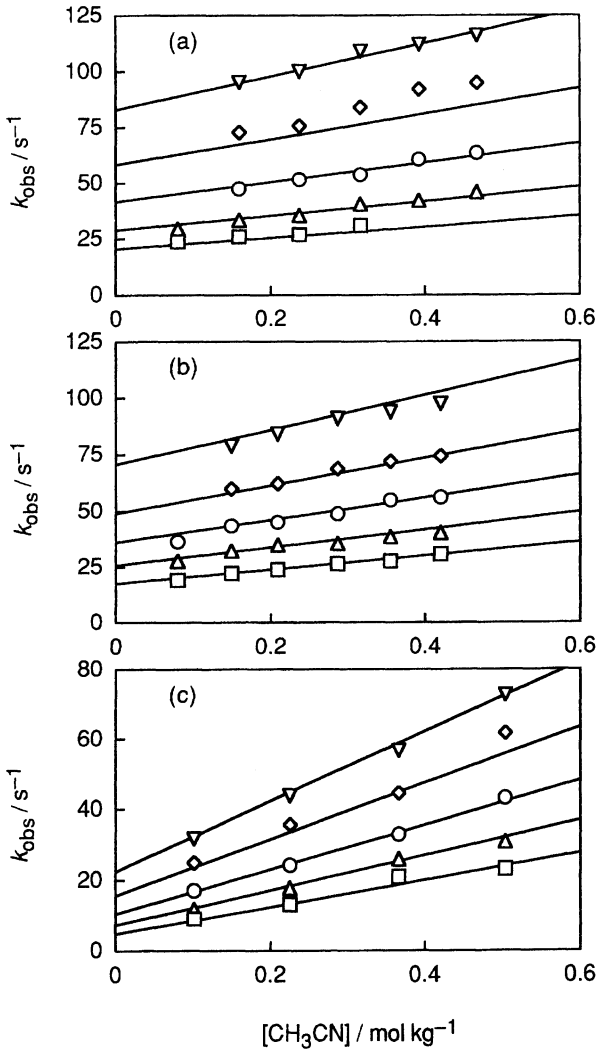

Fig. 5. (a) Dependence of k_{obs} for **1** on the concentration of free CH_3CN, $[CH_3CN]$, at 289.2 K (□), 293.0 K (△), 297.2 K (○), 301.1 K (◇), 305.3 K (▽); [Pd complex]=3.0×10^{-2} mol kg^{-1}, $C_{CF_3SO_3^-}$ =0.39 mol kg^{-1}. (b) Dependence of k_{obs} for **2** on the concentration of free CH_3CN, $[CH_3CN]$, at 309.3 K (□), 313.4 K (△), 317.1 K (○), 320.6 K (◇), 324.8 K (▽); [Pd complex]=5.0×10^{-2} mol kg^{-1}, $C_{CF_3SO_3^-}$ =0.34 mol kg^{-1}. (c) Dependence of k_{obs} for **3** on the concentration of free CH_3CN, $[CH_3CN]$, at 313.2 K (□), 317.3 K (△), 321.1 K (○), 325.1 K (◇), 328.9 K (▽); [Pd complex]= 8×10^{-2} mol kg^{-1}, $C_{BF_4^-}$ =0.8 mol kg^{-1}. The solid lines are depicted by using the values of activation parameters.

amine ligands and the electrostatic interaction between the counter anion and bound ligand as observed in the variation of the ^1H NMR chemical shifts. Actually, the present tridentate amine ligands intrinsically have a large bound ligand effect in comparison with the bound acetonitrile because of their strong basicity. Furthermore, the deshielding amine protons due to the ion-pair formation enhance the basicity of the amine nitrogens. It is worthwhile noticing the difference in the effect of the counter anion on the k_1 path by comparison between **2** and **3** which have the dien ligand in common. The rate constant for the k_1 path at 25 °C for **2** is larger than that

Table 7. Exchange Rate Constants and Activation Parameters for Acetonitrile Exchange on Pd(II) Complexes

	k_1 path			k_2 path			
	k_1^{298} / s^{-1}	$\Delta H_1^{\ddagger}$ / kJ mol^{-1}	$\Delta S_1^{\ddagger}$ / J K^{-1} mol^{-1}	k_2^{298} / kg mol^{-1} s^{-1}	$\Delta H_2^{\ddagger}$ / kJ mol^{-1}	$\Delta S_2^{\ddagger}$ / J K^{-1} mol^{-1}	
1	44.5	61.2±4.4	−8±15	54.8	48±13	−52±44	This work
2	5.75	72.2±3.1	12±10	15.6	46.6±8.2	−66±26	This work
3	0.904	82.2±8.2	30±25	14.2	49.5±5.5	−57±17	This work
$[Pd(CH_3CN)_4](BF_4)_2$				48.8	45.4±0.8	−60.1±2.4	a)

a) Ref. 1d.

for **3** by a factor of about six, mainly due to a smaller $\Delta H_1^{\ddagger}$ value for **2**. Such enhancement of the k_1 path is ascribed to the stronger hydrogen bonding of $CF_3SO_3^-$ with amine protons in comparison with BF_4^-. This difference in hydrogen bonding is well reflected in the chemical shifts of the amine protons by the ion-pair formation, i.e., the downfield shift for the amine protons of **2** is much more remarkable than that of **3** (Table 6).

The rate constant at 25 °C for the associative k_2 path for the dptn complex **1** is apparently larger than those for the dien complex, **2** and **3**, which are comparable at 25 °C (Table 7). The stronger basicity of dptn rather than dien should be a disadvantage to the associative mechanism because an increase in electron density on the central Pd(II) ion inhibits the associative attack of an entering ligand. Accordingly, the promotion of the k_2 path for **1** is attributed to greater flexibility of the large chelate ring of dptn compared with that of dien. The bonds between the central Pd(II) ion and the donor nitrogens should be more extended in the five-coordinate transition state than in the four-coordinate ground state because of an increase in electronic repulsion. Therefore, the larger chelate ring of the dptn ligand can more flexibly form the structure required in the associative transition state for the k_2 path, compared with that of the dien ligand.

This work was supported by Grants-in-Aid for Scientific Research Nos. 06640779, 07454199, and 07504003 from the Ministry of Education, Science, Sports and Culture. S. A. gratefully acknowledges the Kurata Foundation for support.

References

1) a) L. Helm, L. I. Elding, and A. E. Merbach, *Helv. Chim. Acta*, **67**, 1453 (1984); b) B. Brönnum, H. S. Johansen, and L. H. Skibsted, *Acta Chem. Scand.*, **43**, 975 (1989); c) J. Berger, M. Kotowski, R. van Eldik, U. Frey, L. Helm, and A. E. Merbach, *Inorg. Chem.*, **28**, 3759 (1989); d) N. Hallinan, V. Besançon, M. Forster, G. Elbaze, Y. Ducommun, and A. E. Merbach, *Inorg. Chem.*, **30**, 1112 (1991); e) U. Frey, S. Elmroth, B. Moullet, L. I. Elding, and A. E. Merbach, *Inorg. Chem.*, **30**, 5033 (1991); f) Y. Ducommun, L. Helm, A. E. Merbach, B. Hellquist, and L. I. Elding, *Inorg. Chem.*, **28**, 377 (1989).

2) a) G. Alibrandi, D. Minniti, L. Monsù Scolaro, and R. Romeo, *Inorg. Chem.*, **28**, 1939 (1989), and references therein; b) D. Minniti, *J. Chem. Soc., Dalton Trans.*, **1993**, 1343.

3) a) D. Minniti, *Inorg. Chem.*, **33**, 2631 (1994); b) G. Alibrandi, D. Minniti, L. Monsù Scolaro, and R. Romeo, *Inorg. Chem.*, **27**, 318 (1988), and references therein.

4) S. Aizawa, T. Yagyu, and S. Funahashi, *Chem. Lett.*, **1993**, 1607. The ion-pair formation constant K_1 was obtained by applying a least-squares fitting to the following equations:

$$\delta_{obs} = \delta_{free} - (\delta_{free} - \delta_{ip})K_1[BF_4^-]/(1 + K_1[BF_4^-])$$
$$[BF_4^-] = [K_1C_{BF_4^-} - K_1C_{Pd} - 1 + \{(K_1C_{BF_4^-} - K_1C_{Pd} - 1)^2 + 4K_1C_{BF_4^-}\}^{1/2}]/2K_1$$

where δ_{obs} is the observed chemical shift of the amine proton, δ_{free} and δ_{ip} are the chemical shifts of the free and 1 : 1-ion-pairing amine proton, respectively, and C_{Pd} is the total concentration of the Pd(II) complex.

5) A. Arthur, W. M. Haynes, and L. P. Varga, *Anal. Chem.*, **38**, 1630 (1966).

6) S. Funahashi, "High Pressure Liquids and Solutions," ed by Y. Taniguchi, M. Senoo, and K. Hara, Elsevier, Amsterdam (1994), pp. 31—48.

7) The programs used were modified versions of Main, Hull, Lessinger, Declerg, and Woolfson's MULTAN82 and Johnson's ORTEP II.

8) The program used was Scheidt and Haller's (Notre Dame) version of Busing and Levy's ORFLS.

9) "International Tables for X-Ray Crystallography," Kynoch Press, Birmingham (1974).

10) The tables of the anisotropic temperature factors for non-hydrogen atoms, bond distances and angles, the parameters of hydrogen atoms and the $F_o - F_c$ are deposited as Document No. 69041 at the Office of the Editor of Bull. Chem. Soc. Jpn.

11) M. E. Cradwick, D. Hall, and R. K. Phillips, *Acta Crystallogr., Sect. B*, **B27**, 480 (1971).

12) R. J. H. Clark, V. B. Croud, H. M. Dawes, and M. B. Hursthouse, *J. Chem. Soc., Dalton Trans.*, **1986**, 403.

13) A. Vacca, D. Arenare, and P. Paoletti, *Inorg. Chem.*, **5**, 1384 (1966).

14) J. W. Allison and R. J. Angelici, *Inorg. Chem.*, **10**, 2233 (1971).

15) J. A. Riddick, W. B. Bunger, and T. K. Sakano, "Organic Solvents," 4th ed, John Wiley & Sons, New York (1978).